Development and characterisation of buparvaquone nanosuspensions for pulmonary delivery in the treatment of *Pneumocystis* pneumonia

Inaugural-Dissertation

to obtain the academic degree

Doctor rerum naturalium (Dr. rer. nat.)

submitted to the Department of Biology, Chemistry and Pharmacy of the Freie Universität Berlin

by

NORMA HERNANDEZ-KIRSTEIN

from Mexico

Berlin, November 2006

1st Reviewer: Prof. Dr. Rainer H. Müller

2nd Reviewer: Prof. Dr. Udo Bakowsky

Date of defence: December 13th 2006

To my family with plenty of love and gratitude



INDEX OF CONTENTS

	INDEX OF CONTENTS	i
	LIST OF FIGURES	vii
	LIST OF TABLES	xii
	ABBREVIATIONS	. xiv
1.	INTRODUCTION, AIMS AND OBJECTIVES	1
	1.1 Introduction	2
	1.2 Aims and objectives	4
	1.2.1 Formulation development	4
	1.2.2 In vitro application of buparvaquone formulations	4
	1.2.3 Buparvaquone solid dispersions	5
	1.2.4 In vivo application of buparvaquone nanosuspensions	5
2.	LITERATURE REVIEW	7
	2.1 The concept of nanocrystals as delivery system of lipophilic drugs	8
	2.1.1 Definition and history	8
	2.1.2 Saturation solubility	9
	2.1.3 Reduction in particle size and dissolution velocity	9
	2.1.4 Overview of current applications	. 10
	2.1.4.1 Oral delivery	. 10
	2.1.4.2 Intravenous delivery	. 10
	2.1.4.3 Inhaled delivery	. 11
	2.2 Pulmonary anatomy and physiology	11
	2.2.1 Anatomy and passage of particles through the airways	. 11
	2.2.1.1 The nose	. 11
	2.2.1.2 The nasopharynx	. 12
	2.2.1.3 The larynx	. 12
	2.2.1.4 The trachea and the lower airways	. 12
	2.2.2 Physiology	. 13
	2.3 General aspects related to pulmonary drug delivery	14
	2.3.1 Market perspective	. 15
	2.3.2 Mechanisms of aerosol deposition in the lung and the aerodynamic	size
	distribution of inhaled particles	. 16
	2.3.2.1 Inertial impaction	. 16

2.3.2.2 Sedimentation (settling)	17
2.3.2.3 Diffusion (Brownian motion)	17
2.3.2.4 Interception	17
2.3.3 Factors affecting drug deposition	18
2.3.3.1 Properties of the aerosol	18
2.3.3.2 Lung morphology	18
2.3.3.3 Breathing pattern	18
2.3.4 Mechanisms of drug absorption in the lung	19
2.3.4.1 Transcellular diffusion	19
2.3.4.2 Paracelullar diffusion	19
2.3.4.3 Carrier mediated transport	20
2.4 Current formulations and devices for oral inhalation of poorly water so	luble
drugs	20
2.4.1 Aqueous suspensions for nebulization	20
2.4.2 Suspensions for pressurized Metered Dose Inhalers (pMDI's)	21
2.4.3 Powders and solid dispersions for use with Dry Powder Inhalers (DPI's) . 22
2.5 Nebulization	23
2.5.1 Basic principles of atomisation theory	24
2.5.1.1 Generation of particles with ultrasonic nebulization	24
2.5.1.2 Generation of particles with vibrating orifice ultrasonic nebulization	25
2.5.1.3 Generation of particles with jet nebulization	25
2.5.2 Types of nebulizers	26
2.5.2.1 Jet nebulizers	26
2.5.2.2 Ultrasonic nebulizers	27
2.5.2.3 Electrical nebulizers	28
2.5.2.4 New "mixed" nebulizers	29
2.5.3 Factors affecting nebulizer performance	29
2.5.3.1 Humidity and temperature of ambient air	29
2.5.3.2 Baffles	30
2.5.3.3 Characteristics of the solution	30
2.5.3.4 Solution volume or fill volume	30
2.5.3.5 Operating time	30
2.5.3.6 Air pressure to the jet	30
2.5.3.7 Dead volume	31

	2.5.4 Problems with conventional dispersions during nebulization of lipop	hilic
	drugs	. 31
	2.6 Pneumocystis pneumonia	32
	2.6.1 Aetiology and epidemiology	. 32
	2.6.2 Current drugs used for prophylaxis and therapy	. 36
3.	MATERIALS AND METHODS	. 37
	3.1 Materials	38
	3.1.1 Buparvaquone	. 38
	3.1.2 Atovaquone	. 40
	3.1.3 Parvaquone	. 41
	3.1.4 Emulsifying agents	. 42
	3.1.4.1 Tyloxapol [®]	. 42
	3.1.4.2 Poloxamer 188	. 43
	3.1.4.3 Polyvinyl alcohol	. 43
	3.1.4.4 Purified soy lecithin	. 44
	3.1.4.5 Sodium glycocholate	. 45
	3.1.4.6 Tween [®] 80	. 45
	3.1.5 Other materials	. 46
	3.1.5.1 Polyvinyl pyrrolidone	. 46
	3.1.5.2 Inulin	. 46
	3.1.5.3 Glycerol	. 47
	3.1.5.4 Water	. 48
	3.1.5.5 Nebulizer systems	. 48
	3.2 Methods	50
	3.2.1 Production of nanosuspensions with high pressure homogenisation	. 50
	3.2.1.1 Operation principle of a piston-gap type high pressure homogeniser	. 50
	3.2.1.2 Preparation of Nanosuspensions	. 51
	3.2.2 Characterization of drug nanosuspensions: size distribution, crystal na	ture
	and zeta potential	. 52
	3.2.2.1 Laser Diffractometry (LD)	. 52
	3.2.2.2 Photon Correlation Spectroscopy (PCS)	. 54
	3.2.2.3 Zeta potential and Laser Doppler Anemometry (LDA)	. 55
	3.2.2.4 Polarized light microscopy	. 56
	3.2.2.5 X-Ray Diffraction	. 57

	3.2.2.6 Scanning Electron Microscopy (SEM)	58
	3.2.2.7 Viscosity and density	58
	3.2.2.8 Surface tension	59
	3.2.2.9 In vitro dissolution tests for nanosuspensions	59
	3.2.2.10 HPLC method to determine the content of buparvaquone	60
3	.2.3 Methods used during the in vitro characterisation of aerosol produc	ced
d	uring the nebulisation of nanosuspensions	61
	3.2.3.1 Cascade Impaction Analysis	62
	3.2.3.2 Laser diffraction analysis	65
	3.2.3.3 Investigation of drug nanocrystals aggregation	69
	3.2.3.4 Drug output from jet nebulizers	70
3	.2.4 Methodology employed during the in vivo tests for the inhalation	of
b	uparvaquone nanosuspensions by Pneumocystis pneumonia infected mice	71
	3.2.4.1 Laboratory animals	71
	3.2.4.2 Development of Pneumocystis pneumonia infection	72
	3.2.4.3 Calculation of the dose inhaled and definition of inhalation expos	ure
	times	73
	3.2.4.4 Test procedure for the drugs administration	74
	3.2.4.5 Histological and staining methods for microscopy	74
	3.2.4.6 Technique for estimating Pneumocystis burden in the lung	75
	3.2.4.7 HPLC method to quantify buparvaquone in mice plasma	75
	3.2.4.8 HPLC method to quantify buparvaquone in mice organs	76
	3.2.4.9 Evaluation of drug activity	77
3	.2.5 Preparation of buparvaquone solid dispersions	79
	3.2.5.1 Spray drying process (SD)	80
	3.2.5.2 Spray-freeze drying process (SFD)	80
3	.2.6 Characterization of buparvaquone solid dispersions	81
	3.2.6.1 Scanning Electron Microscopy (SEM)	81
	3.2.6.2 Temperature Modulated Differential Scanning Calorimetry (TMDSC)	81
	3.2.6.3 X-Ray Powder Diffraction (XRPD)	81
	3.2.6.4 Dynamic Vapour Sorption (DVS)	82
	3.2.6.6 In vitro dissolution behaviour	82
	3.2.6.7 Quantification of PVP during dissolution tests	83

4. RESULTS AND DISCUSSIONS	85
4.1 Nanosuspensions for inhalation. Development and nebulization behaviour	r 86
4.1.1 Development, follow up stability and dissolution studion	es of
buparvaquone nanosuspensions	86
4.1.1.1 Optimisation of the number of homogenisation cycles	86
4.1.1.2 Formulation screening with different dispersion media and fol	low-up
stability	88
4.1.1.3 Crystallinity of the nanosuspensions	97
4.1.1.4 Saturation solubility of buparvaquone nanocrystals	99
4.1.1.5 In vitro dissolution behaviour of buparvaquone nanocrystals	100
4.1.2 Nebulization performance	101
4.1.2.1 Droplet size in aerosols	101
4.1.2.2 Analysis of drug nanocrystals	107
4.1.3 Drug output from jet nebulizers	111
4.1.3.1 Theoretical calculation of the nanocrystals load per aerosol drople	et112
4.1.3.2 The effect of the physicochemical properties of the dispersion me	dia on
the droplet size distribution of jet nebulizers	115
4.1.3.3 Drug nanocrystals aggregation with Pari LC Star nebulizer	120
4.1.4 Conclusions	121
4.2 Inhalation of buparvaquone nanocrystals in the therapy of pneumon	ocystis
pneumonia infected mice	122
4.2.1 Physical and microbiological characterization of the buparva	ıquone
nanosuspension	122
4.2.2 Particle size distribution of the atovaquone suspension	123
4.2.3 Characterization of the aerosol distribution and nebulizer performance	e124
4.2.4 Drug distribution after specified inhalation exposure times	124
4.2.5 Responses to treatment of <i>Pneumocystis</i> pneumonia among groups .	126
4.2.6 Conclusion	135
4.3. Nanocrystals in the solid state for pulmonary delivery	136
4.3.1 Preparation of the solid dispersions	136
4.3.2 Degree of crystallinity and thermodynamical characteristics of the po	owders
	138
4.3.3 Water vapour absorption into solid dispersions/solutions	141
4.3.4 Morphology and structure of the powders	144

4.3.4 Dissolution behaviour: Mechanisms of drug release	151
4.3.6 Conclusion	154
5. SUMMARY/ ZUSAMMENFASSUNG	155
5.1 Summary	156
5.2 Zusammenfassung	159
6. REFERENCES	163
6. References	164
7. APPENDICES	185
7.1 APPENDIX A: Size distribution of the nanosuspension formulations n	neasured
with LD and PCS techniques during Follow-up stability studies (Mean ± S	SD, n=3).
	186
7.2 APPENDIX B: LD diameters of aerosol droplets (mean ± SD; n=5) p	oroduced
with with jet and ultrasonic nebulization of Formulations A, B and referer	nces 1, 2
and 3 (see section 4.1.2.1)	192
AKNOWLEDGEMENTS	196
CURRICULUM VITAE	198
DUDUICATIONS LIST	100

LIST OF FIGURES

		<u>Page</u>
Figure 2-1:	Main mechanisms of aerosol deposition in the lung	16
Figure 2-2:	Example of an enhanced jet nebulizer showing the aerosol flow during inspiration and expiration phases	27
Figure 2-3:	Pneumocystis life cycle	35
Figure 3-1:	Chemical structure of buparvaquone	39
Figure 3-2:	Chemical structure of atovaquone	40
Figure 3-3:	Structural formula of parvaquone	41
Figure 3-4:	Chemical structure of Tyloxapol®	43
Figure 3-5:	Molecular formula of Poloxamer 188	43
Figure 3-6:	Molecular formula of Polyvinyl Alcohol	44
Figure 3-7:	Chemical structure of phosphatidylcholine	45
Figure 3-8:	Chemical structure of Tween®80	45
Figure 3-9:	Chemical structure of Polyvinyl Pyrrolidone	46
Figure 3-10:	Chemical structure of inulin	47
Figure 3-11:	Representation of the set-up of a laser diffraction instrument. Adapted from the international standard ISO 13320-1	53
Figure 3-12:	(a) External view of the whole body inhalation chamber Glas-Col [®] Model A4224. (b) Diagram explaining the components and aerosol flow inside of the chamber (Glas-Col [®] 2000)	63
Figure 3-13:	Photograph of the assembled 8-stage Andersen Cascade Impactor (ACI-8). On the right side, a view of the individual components: separation stages and collection plates	64
Figure 3-14:	Representation of the set-up of a laser diffraction instrument to measure droplet size of the aerosolized nanosuspensions	67
Figure 3-15:	Photograph of the laser diffraction apparatus Sympatec Helos BF/Magic [®] , with a modular inhaler adapter (INHALER [®] 2000)	69
Figure 3-16:	Representative photos of the different infection rates (1 to 4) defined for the evaluation of the lung smears prepared from the 5 groups of treated animals. Diff-Quik® stain, 200× magnification	78
Figure 4-1:	LD diameters d50%, d90%, d95% and d99% obtained along a 60 cycles homogenisation process at 1500 bar. Dispersion medium is an aqueous solution of 0.5% poloxamer 188	87

Figure 4-2:	Z-Average and polydispersity index (PI) values obtained along a 60 cycles homogenisation process at 1500 bar. Dispersion medium is an aqueous solution of 0.5% poloxamer 188	88
Figure 4-3:	Particle size distribution of the drug nanocrystals in formulations A-E measured at the day of production and after 1, 3 and 6 months of storage time at room temperature. Size distribution was measured with PCS (a) and LD (b) techniques	90
Figure 4-4a	Z Average particle diameter and polydispersity indices measured with PCS technique. Formulations E, F and G contain 1, 2 and 7 % of drug respectively	91
Figure 4-4b	LD particle diameter measured for formulations E, F and G contain 1, 2 and 7 % of drug respectively along 6 months storage time	92
Figure 4-5	Particle size distribution of the drug nanocrystals in formulation H measured at the day of production and after 1, 3 and 6 months of storage time at room temperature and under refrigeration. Size distribution was measured with PCS (a) and LD (b) techniques	93
Figure 4-6	Particle size distribution of the drug nanocrystals in formulation I-K measured at the day of production and after 1, 3 and 6 months of storage time at room temperature. Size distribution was measured with PCS (a) and LD (b) techniques	94
Figure 4-7:	SEM Photographs of buparvaquone original (upper) and nanosuspension after 40 homogenisation cycles (lower). Homogenisation at 1500 bar, room temperature	97
Figure 4-8:	X-Ray diffractogram of buparvaquone nanosuspension formulation H after 5(a), and 40 (b) homogenisation cycles. A placebo formulation is shown in (c). Capillary sample holder was used for the measurement of the aqueous dispersion.	98
Figure 4-9:	Dissolution test of buparvaquone nanocrystals and original powder (LD d50% = $86.5 \pm 9.0 \mu m$) using 2%Tween 80 solution as a dissolution medium.	100
Figure 4-10:	Size distribution obtained after nebulizing nanosuspension A using Respi-jet Kendall nebulizer and Pari Turbo Boy nebulizer (top and center) and nanosuspension B using Pari Turbo Boy nebulizer (bottom). All compared vs. the dispersion solution alone	104

Figure 4-11:	LD diameters characterizing the size distributions of nanosuspension Form A nebulized with nebulizer Multisonic at the beginning (left), middle (center) and end (right) of the nebulization period, LD diameters d50%, d90%, d95% and d99%	105
Figure 4-12:	Characterization LD parameters diameters 50%, 90%, 95%, 99% of size distributions of nebulized suspension A with the nebulizers Respi-jet Kendall (A), Pari Turbo Boy (B), Multisonic (C), Omron U-1 (D). Sizes analysed at the beginning of the nebulization period	106
Figure 4-13:	LD size distribution of drug nanosuspension A (left) and nanosuspension B (right) nebulized with nebulizer Pari Turbo Boy. Size distributions analysed at the beginning of the nebulization process	107
Figure 4-14:	LD size distribution of the original drug nanosuspension (left) and drug nanosuspension A after the nebulization with the Pari Turbo Boy nebulizer, droplets were collected in the first half of the nebulization time (minute $0-2.5$)	108
Figure 4-15:	LD characterization parameters diameters 50%, 90%, 95% and 99% of suspension A in the reservoir of the nebulizer Pari Turbo Boy (left) and the nebulizer Omron U1 (right) at the end of the nebulization process compared to nanosuspension before nebulization.	109
Figure 4-16:	PCS diameters and polidispersity indexes of the drug nanosupension B before and after its nebulization by Respi-jet Kendall nebulizer (A), Pari Turbo Boy nebulizer (B), Multisonic nebulizer (C) and Omron U-1 nebulizer (D)	110
Figure 4-17:	PCS diameters and polidispersity indexes (PI) of nanosuspension A as a function of nebulization time (1 min, 2,5 min, 5 min), Pari Turbo Boy nebulizer (left) and Multisonic nebulizer (right)	111
Figure 4-18:	Graphic representation of the distribution of microcrystals (left) and of nanocrystals (right) in aerosol droplets	112
Figure 4-19:	Percentages of drug emitted obtained with different nanosuspension formulations using a Pari LC Star nebulizer. (a) Represents the influence of viscosity and (b) the influence of the surface tension values on the quantity of drug emitted	119
Figure 4-20:	Influence of the nebulization process on particle size diameter using Pari LC Star and formulations C-D. PCS and LD particle diameter are shown at the beginning (1), at the end (3) of the nebulization and the diameter of particles detected in the aerosol collected (2)	120

Figure 4-21:	Distribution of aerosolized buparvaquone in different mouse tissues. One mouse per exposure time. A second experiment following identical procedures gave essentially the same results (data not shown). Plasma values in µg drug per ml plasma.	125
Figure 4-22:	Pneumocystis burden as microscopically determined in lung homogenate preparations using the bisBenzimide stain	127
Figure 4-23:	Pneumocystis infection score as microscopically determined (magnification 200x) in lung impression smears stained with BB (a) and DQ (b)	129
Figure 4-24a:	Comparison between trophozoite clusters in lung impression smears stained with DQ. Infected animals were left untreated (upper) or were treated with BPQ per os (lower). Magnification 400x. Pictures show trophozoit clusters of the parasite (TC), erythrocytes (E) and host cells (C)	131
Figure 4-24b:	Comparison between trophozoite clusters in lung impression smears stained with BB. Infected animals were left untreated (upper) or were treated with BPQ per os (lower). Magnification 400x. Pictures show trophozoit clusters of the parasite (TC), erythrocytes (E) host cells (C) and intact trophozoits	132
Figure 4-25:	Details of lung morphology typically observed in <i>P. murina</i> -infected RAG mice after 3 weeks of therapy	134
Figure 4-26:	Crystallinity and grade of miscibility investigations for PVP solid dispersions/solutions prepared with BPQ	139
Figure 4-27:	XRPD studies of BPQ incorporated into inulin solid dispersions	141
Figure 4-28:	Dynamic vapour sorption (DVS) studies of the BPQ powders prepared with carrier PVP (a) and inulin (b)	143
Figure 4-29a:	SEM picture of the buparvaquone powder particles in the sample I-A-SFD. A mixture of TBA drug solution and aqueous inulin solution was spray-freeze dryed. Hollow particles were formed with small nanocrystals incorporated between the sugar net (arrow). Magnification 7500 x	144
Figure 4-29b:	SEM picture of the buparvaquone powder particles in the sample I-B-SFD. A half diluted mixture of TBA drug solution and aqueous inulin solution was spray-freeze dryed. Hollow particles were formed with small nanocrystals incorporated between the sugar net (arrow). Magnification 7500 x	145
Figure 4-29c:	SEM picture of the buparvaquone powder particles in the sample PVP-A-SFD. A mixture of TBA drug solution and TBA solution of PVP was spray-freeze dryed. Sponge-like particles were formed. Magnification 7500 x	146

Figure 4-29d:	SEM picture of the buparvaquone powder particles in the sample PVP-B-SFD. A mixture of TBA drug solution and aqueous solution of PVP was spray-freeze dryed. Highly porous particles were formed. Magnification 7500 x	147
Figure 4-29e:	SEM picture of the buparvaquone powder particles in the sample I-NC-SFD. A mixture of BPQ nanosuspension and aqueous solution of inulin was spray-freeze dryed. Aggregates of undefined structure were formed. Drug nanocrystals can be distinguished (arrow). Magnification 7500 x	148
Figure 4-29f:	SEM picture of the buparvaquone powder particles in the sample I-NC-SFD. A mixture of BPQ nanosuspension and aqueous solution of inulin was spray-freeze dryed. Aggregates of undefined structure were formed. Drug nanocrystals can be distinguished (arrow). Magnification 7500 x	149
Figure 4-29g:	SEM picture of the buparvaquone powder particles in the sample I-NC-SD. A mixture of BPQ nanosuspension and aqueous solution of inulin was spray dryed. Rounded particles were formed. Magnification 7500 x	150
Figure 4-29h:	SEM picture of the buparvaquone powder particles in the sample PVP-NC-SD. A mixture of BPQ nanosuspension and aqueous solution of PVP was spray dryed. Shrinkage particles were formed. Magnification 7500 x	150
Figure 4-30:	BPQ release curves of the PVP powders prepared	151
Figure 4-31:	BPQ release curves of the inulin powders prepared	153

LIST OF TABLES

	<u>Page</u>	
Table 2-1:	pMDI's marketed products based in dispersion formulations.	21
Table 2-2:	Examples of DPI's currently in the market and their mechanism of action	23
Table 3-1:	Nebulization systems used to test nanosuspensions	49
Table 4-1:	Formulation composition of the nanosuspensions prepared for pulmonary administration	89
Table 4-2:	Zeta potential values for the buparvaquone nanosuspensions selected due to their good stability. Measurements were performed in adjusted 50 μ S/cm Milli-Q water and pH 6.0-7.0	95
Table 4-3:	Drug content of physically stable nanosuspension formulations at the day of production and after 6 months of storage. Measurements performed with HPLC method. Values represent the mean ± SD of 3 measurements	96
Table 4-4:	Saturation solubility values for the buparvaquone nanosuspensions selected. Measurements were performed using HPLC method PCS particle diameters of the drug nanocrystals are also summarized	99
Table 4-5:	Composition of buparvaquone nanosuspension A and B used for nebulization study	101
Table 4-6:	Particle size characterization (mean \pm SD, n=3) of buparvaquone nanosuspension A and B used for nebulization study	102
Table 4-7:	Theoretical calculations to determine the maximum BPQ nanocrystals (400 nm) load in 2.8 μ m aqueous droplets. The maximum of microcrystals (2 μ m) load in the same size droplets are calculated for comparison	113
Table 4-8:	Theoretical calculations to determine the nanocrystals load in aerosol droplets produced with a 5% nanosuspension	114
Table 4-9:	Composition of buparvaquone nanosuspensions used with Pari LC Star jet nebulizer	116
Table 4-10:	Aerosolization characteristics of different nanosuspension formulations following nebulization with Pari LC Star nebulizer. A fill volume of 5 mL was used in all the cases	117
Table 4-11:	Particle size distribution of Wellvone® as supplied and after dilution. Measurements were performed with a laser diffractometer	123

Table 4-12:	Summary of the composition and manufacture processes used in the preparation of the solid dispersions	136
Table 4-13:	Particle diameter values measured with PCS and LD. Aqueous dispersion of drug nanocrystals were stabilized adding 0.5 % poloxamer 188	137

ABBREVIATIONS

SXT Trimethoprim and Sulfamethoxazole

ATQ Atovaquone

BPQ Buparvaquone

PcP Pneumocystis pneumonia

HAART Highly Active Antiretroviral Therapy

HIV Human Immunodeficiency Virus

AIDS Acquired Immunodeficiency Syndrome

DPI Dry Powder Inhaler

pMDI Pressurized metered dose inhaler

HLB Hydrophilic-lipophilic balance

PVA Polyvinyl alcohol

PVP Polyvinyl pyrrolidone

DPPC Dipalmitoylphosphatidylcholine

FDA Food and Drug Administration Office (US Government)

GRAS Generally Recognized As Safe

LD Laser Diffractometry

PCS Photon Correlation Spectroscopy

PI Polydispersity Index

LDA Laser Doppler Anemometry

NaCl Sodium chloride

XRPD X-Ray powder diffraction

SEM Scaning Electron Microscope

MMAD Mass Median Aerodynamic Diameter

GSD Geometric Standard Deviation

MMD Mass Median Diameter

ACI Andersen Cascade Impactor

VMD Volume Median Diameter

DQ Diff-Quik[®] stain

BB Bis-benzimide stain

H&E Hematoxylin and eosin stain
HBSS Hank's balanced salt solution

HPLC High pressure liquid chromatography

OIF Oild immersion field

SFD Spray-freeze drying process

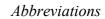
SD Spray drying process

TMDSC Temperature Modulated Differential Scanning Calorimetry

DVS Dynamic vapour sorption

T_g' Transicion glass temperature

NS Nanosuspension TBA Ter-butyl alcohol



(INTENTIONALLY BLANK)